

Magnetorotons in Moiré Fractional Chern Insulators

Xiaoyang Shen,^{1,*} Chonghao Wang,^{1,*} Xiaodong Hu,^{2,*} Ruiping Guo,^{1,3}
Hong Yao,³ Chong Wang,^{1,†} Wenhui Duan,^{1,3,4,5,‡} and Yong Xu^{1,4,6,§}

¹State Key Laboratory of Low Dimensional Quantum Physics and
Department of Physics, Tsinghua University, Beijing, 100084, China

²Department of Material Science and Engineering,
University of Washington, Seattle, WA 98195, USA

³Institute for Advanced Study, Tsinghua University, Beijing 100084, China

⁴Frontier Science Center for Quantum Information, Beijing, China

⁵Beijing Academy of Quantum Information Sciences, Beijing 100193, China

⁶RIKEN Center for Emergent Matter Science (CEMS), Wako, Saitama 351-0198, Japan

(Dated: December 3, 2024)

We perform a comprehensive study of the intraband neutral excitations in fractional Chern insulators (FCIs) within moiré flatband systems, particularly focusing on the twisted transition metal dichalcogenide homobilayers. Our work provides a detailed description of the magnetorotons in FCIs utilizing exact diagonalization. We further explore the nature of the geometrical excitations in the long-wavelength limit, identifying chiral angular momentum-2 features. Additionally, we find that these modes exhibit chiral mixing and become unstable as the FCI deviates from its ideal conditions. Interestingly, we find evidence of the nonchiral geometrical excitations in the charge density wave (CDW), demonstrating that the geometrical excitations might be supported even in the absence of topology. Our work sheds light on the profound interplay between geometry and topology from the perspectives of excitations.

Introductions.— Moiré materials based on multilayer van de Waals materials have recently become a burgeoning area with considerable interest in the emergence of remarkable phases [1–13]. Among the strongly-correlated states, fractional Chern insulators (FCIs) holds a broad appeal, for its novel nature and the potential for quantum computation [14, 15]. FCIs can be considered as a zero-field, lattice analogy of the fractional quantum Hall (FQHs) state, henceforth inheriting the intrinsic topological nature of FQHs. In realistic systems, deviations from ideal flat bands and more complex correlated effects give rise to emergent physics in FCIs that extends beyond the conventional lowest Landau level (LLL) framework [16–24]. Numerous theoretical studies [25–32] have predicted that FCIs manifest in moiré materials, such as twisted bilayer graphene (TBG) and twisted bilayer transition metal dichalcogenides (TMDs). These predictions have since been corroborated by experimental observations. [5, 33–39]. While most researches have focused on the ground state that straightforwardly encode the topological order, the low-lying collective excitations that could convey the information of the topological and geometrical properties of FCIs remain largely unknown [40–42].

One of the celebrated hallmarks in FQHs is the existence of intraband neutral excitations, or *magnetorotons* proposed by Girvin, MacDonald, and Platzman (GMP) [43]. These neutral excitations can be effectively described using a density wave ansatz within the framework of the single mode approximation (SMA). The SMA serves as an effective route to capture the behavior of magnetorotons and predict a “roton-like” local minimum at finite momentum. The GMP theory demonstrates that

the dipole transition is entirely inter-LLL, rendering the magnetorotons invisible to the optical detection [44, 45]. By adopting the symmetry analysis or low energy effective theory [46–51], recent studies have revealed that magnetorotons in the long-wavelength limit can be interpreted as excitations of the internal quantum metric. These excitations exhibit a chiral spin-two nature, earning them the name of “massive chiral gravitons.” [52–57]. The remarkable features of geometrical excitations are then observed in experiments several months ago [58–60]. The study of magnetorotons in FQH systems naturally motivates exploration of the similar excitations in FCIs hosted in moiré flatbands. The exceptional tunability of moiré systems enables investigations of magnetorotons not only in ideal FCIs but also in less ideal FCIs and during transitions to other competing phases, where intriguing physics beyond the LLL may emerge.

In this Letter, we provide a comprehensive study of the magnetorotons in FCIs, focusing on the twisted MoTe₂. We extend SMA to FCIs and compute the magnetoroton dispersion. Additionally, we analyze the dynamical response of angular momentum-2 excitations in the long-wavelength limit. In ideal FCIs, these excitations exhibit strongly peaked signals with definite chirality near the zero-momentum magnetoroton energy. However, as the FCI deviates from ideality, the excitations undergo chiral mixing and gradually diminish. When the FCI transitions into a charge density wave (CDW) phase, the magnetoroton softens at specific commensurate momenta corresponding to the density wave. Furthermore, we find evidence of nonchiral angular momentum-2 excitations in the CDW phase. Finally, we propose experimental approaches for detecting these intraband neutral excita-

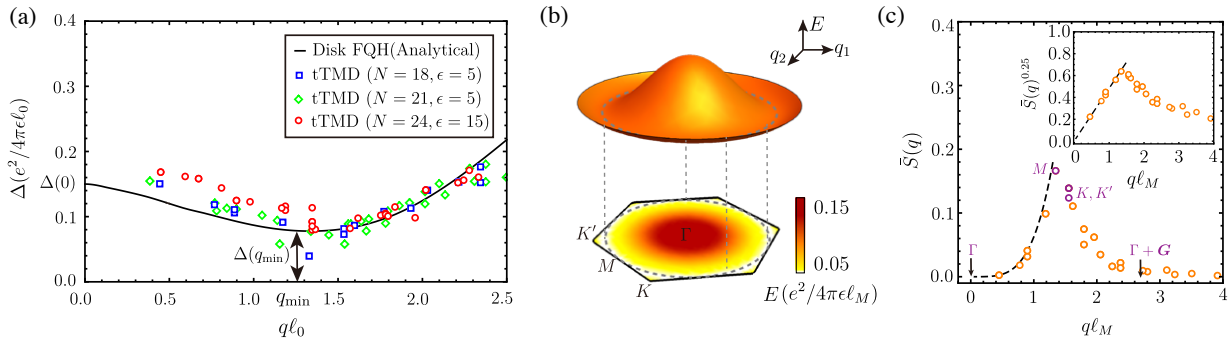


FIG. 1. (a) The rescaling dispersion of the magnetoroton from SMA at $\theta = 3.89^\circ$ and $\nu = -\frac{2}{3}$ filling with different N and ϵ . The black curve is the analytical expression in disk FQHs, directly deduced from the GMP algebra. ℓ_0 represents ℓ_B at FQHs and ℓ_M at FCIs. (b) Three-dimensional diagram illustrating the magnetoroton dispersion. The local minimum resides close to the M points. (c) The projected structure factor $\bar{S}(\mathbf{q})$ at $\nu = -\frac{2}{3}$, $\epsilon = 5$, $\theta = 3.89^\circ$. $\bar{S}(\mathbf{q})$ behaves as $(q\ell_M)^4$ at long-wavelength limit. High symmetry points are labeled in the figure. The inset is the linear fitting of $S^{0.25}(q)$ versus q .

tions, providing a pathway for further exploration.

Model.— We start with the Hamiltonian of twisted MoTe₂

$$\mathcal{H} = \mathcal{H}_0 + V, \quad (1)$$

\mathcal{H}_0 is the single particle moiré Hamiltonian (see Supplemental Material(SM) Sec. I for an explicit description of continuum model), and V is the Coulomb interaction

$$V = \frac{1}{2A} \sum_{\mathbf{q}} V(\mathbf{q}) : \hat{\rho}(\mathbf{q}) \hat{\rho}(-\mathbf{q}) :, \quad V(\mathbf{q}) = \frac{2\pi \tanh(qd)}{\epsilon\epsilon_0 q}, \quad (2)$$

where A is the total area of the system and d is the metallic gate distance and $::$ means normal ordering. $\hat{\rho}(\mathbf{q})$ is the density operator projected to the topmost valence band: $\hat{\rho}(\mathbf{q}) \equiv \sum_{\mathbf{k}} \langle u_{\mathbf{k}+\mathbf{q}} | u_{\mathbf{k}} \rangle \hat{c}_{\mathbf{k}+\mathbf{q}}^\dagger \hat{c}_{\mathbf{k}}$, where $|u_{\mathbf{k}}\rangle$ is the periodic part of Bloch states from the continuum model and $\hat{c}_{\mathbf{k}}^\dagger$ is the creation operator of the Bloch states. Previous studies have revealed that the topmost valence band processes ideal flatness and hosts non-trivial topology simultaneously, further demonstrating its possibility of supporting FCI phases. Recent experiments [33, 35, 38] have found a prominent signal of FCI around the twisted angle $\theta \sim 4^\circ$, the dielectric constant $\epsilon \sim 5 - 15$, and fractional filling $\nu = -\frac{2}{3}$. In the following discussion, we will adopt the parameters that mimic the condition in experiments.

Magnetorotons in ideal moiré FCIs.— Similar to SMA in FQHs, a intraband density wave with momenta \mathbf{q} (GMP wavefunction) in FCIs is constructed as $|\psi_{\mathbf{q}}\rangle = \hat{\rho}(\mathbf{q})|\psi_0\rangle$, $|\psi_0\rangle$ is the many-body ground state from the exact diagonalization and $\hat{\rho}(\mathbf{q})$ is the density operator projected to the topmost band. We focus on the ground state with the lowest energy in the Γ point to erase ambiguity among three-fold degeneracy in the ground states. (See SM Sec. II and Sec. IV for numerical details and relations with other trial wavefunction.)

The variational expectation energy of the excited states is

$$E_{\mathbf{q}} = \frac{\langle \psi_{\mathbf{q}} | H | \psi_{\mathbf{q}} \rangle}{\langle \psi_{\mathbf{q}} | \psi_{\mathbf{q}} \rangle} - E_0 \quad (3)$$

E_0 is the ground state energy of $|\psi_0\rangle$. The dispersion from the SMA approximation in ideal FCIs is shown in Fig. 1. The extrapolation to zero-momentum indicates a gap $\Delta(q=0) \sim 0.17e^2/(4\pi\epsilon\ell_M) \approx 2.125\Delta_{\text{mb}}$, where $\Delta_{\text{mb}} = E_{4\text{th}} - E_{3\text{rd}}$ is the many-body gap separating the degenerated ground states from the excited states. ℓ_M ($\ell_M \equiv \sqrt{3}/4\pi a_M \sim 2\text{nm}$, $a_M \approx a_0/\theta$ is the length of a moiré unit cell) is the characteristic length analogous to the magnetic length ℓ_B ($\ell_B \equiv \sqrt{\hbar/eB} \sim 20\text{nm}$) in FQHs. The zero momentum gap remains robust for various parameters, interaction strengths, and finite-size effects. At small q , we also extracted the projected static structure factor $\bar{S}(q)$. At the long wavelength limit, the projected static structure factor behaves as $(q\ell_M)^4$, which indicates the interband contribution has exhausted all the dipole spectral weight, leading to the vanishing contribution of the optical conductivity from the projected form factor in the ideal band system [61]. There exists a local minimum of the gap at a mediate value of momenta $q_{\text{min}} \sim 1.3/\ell_M$, lying between the M point and the K point in the first BZ, together with the magnetoroton gap $\Delta(q=q_{\text{min}}) \sim 0.08e^2/(4\pi\epsilon\ell_M) \approx \Delta_{\text{mb}}$. At q_{min} , the overlap between the GMP wavefunctions and the exact first excitation state reaches 98.22% at $N = 18$, suggesting the ansatz is effective at q_{min} .

Long-wavelength magnetorotons in ideal FCIs.— So far, the property of long-wavelength magnetorotons remains elusive, since the GMP wavefunctions fail to serve as an effective excitation ansatz at zero momentum. At the long wavelength limit, the dipole spectral weight vanishes as $(q\ell_M)^4$, implying the long-wavelength magne-

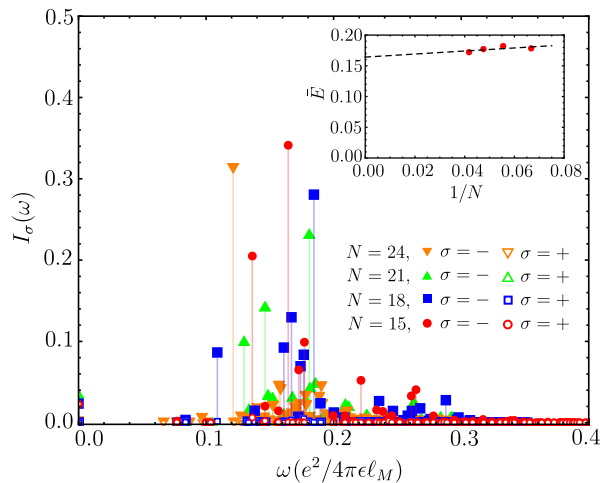


FIG. 2. Spectral weight functions for the angular momentum-2 operators with opposite chiralities in FCI at $\nu = -\frac{2}{3}$, $\epsilon = 5$, $\theta = 3.89^\circ$. Inset is the extrapolation of energy at the large system size limit.

torotons might be angular momentum-2 geometrical excitations associated with the fluctuation of quantum metric [49].

To further elucidate the nature of long-wavelength excitations in FCIs, we numerically investigate the dynamical response to an angular momentum-2 operator coupled to the fluctuation of quantum geometry. All physical excitations transform according to the irreducible representations of the symmetry group. Notice that in the twisted MoTe₂ the symmetry group is D_3 and the displacement field explicitly breaks the symmetry associated with the interchange of layers, reducing the symmetry to C_{3v} [62]. We then utilize the quadratic function (d wave) in the E representations of C_{3v} to probe the angular momentum-2 excitations. Taking account into the translation invariance $\mathcal{T}_1, \mathcal{T}_2$, the underlying form of angular momentum-2 operators with opposite chirality are determined to be [51, 55]

$$\hat{\mathcal{O}}_{\pm}^{(2)} = \sum_{\mathbf{q}} (\mathcal{D}_1(\mathbf{q}) \pm i\mathcal{D}_2(\mathbf{q})) V(\mathbf{q}) : \hat{\rho}(-\mathbf{q}) \hat{\rho}(\mathbf{q}) : \quad (4)$$

where $\mathcal{D}_1(\mathbf{q}) = 2 \cos(\mathbf{a}_1 \mathbf{q}) - \cos(\mathbf{a}_3 \mathbf{q}) - \cos(\mathbf{a}_2 \mathbf{q})$ and $\mathcal{D}_2(\mathbf{q}) = \sqrt{3}(\cos(\mathbf{a}_3 \mathbf{q}) - \cos(\mathbf{a}_2 \mathbf{q}))$, where $\mathbf{a}_1, \mathbf{a}_2$ and $\mathbf{a}_3 = -\mathbf{a}_1 - \mathbf{a}_2$ are unit-cell vectors of lattice. The function $\mathcal{D}_1(\mathbf{q}) \pm i\mathcal{D}_2(\mathbf{q})$ behaves like the chiral d-wave $(q_x \pm iq_y)^2$ at long-wavelength limit [63] (see SM Sec. IV for the construction of the operator).

We now consider the spectral function of operator $\hat{\mathcal{O}}_{\pm}^{(2)}$

$$I_{\pm}^{(2)}(E) = \sum_n |\langle \psi_n | \hat{\mathcal{O}}_{\pm}^{(2)} | \psi_0 \rangle|^2 \delta(E_n - E) \quad (5)$$

$|\psi_0\rangle$ is the ground state and $|\psi_n\rangle$ is the eigenstates. The spectral function is normalized by divided the factor $\langle \psi_0 | \hat{\mathcal{O}}^\dagger \hat{\mathcal{O}} | \psi_0 \rangle$. To directly compare the spectral weight

of different chiralities, we normalize $I_-(E)$ and $I_+(E)$ by $\langle \psi_0 | \hat{\mathcal{O}}^\dagger \hat{\mathcal{O}} | \psi_0 \rangle$. We truncate the summation of eigenstates to ensure that it collects at least 99% of the total spectral weight. We focus on the FCIs states at $\nu = -\frac{2}{3}$, $\epsilon = 5$, $\theta = 3.89^\circ$, as shown in Fig. 2. First of all, over 90% weight of spectral function resides in the region of $0.10 \sim 0.20e^2/(4\pi\epsilon\ell_M)$. As shown in the inset of Fig. 2, the extrapolation to the large system size indicates the excitation energy $\bar{E} = \int d\omega \omega I(\omega) \approx 0.1642e^2/(4\pi\epsilon\ell_M)$, which is close to the long-wavelength magnetoroton energy $\Delta(q=0) \approx 0.17e^2/(4\pi\epsilon\ell_M)$ in SMA. The main body of the figure shows unequivocally that the negative chiral excitations are dominating while the positive chiral excitations are negligible, indicating those excitations are endowed with chiral nature. The results indicate an analogical geometrical property in the ideal FCIs compared with the FQHs.

Neutral excitations in FCI-CDW transitions.— Charge density wave (CDW) is one of FCI's major competitors in moiré systems [64–67]. The intertwinement between the density waves and the intrinsic topology order can give rise to remarkable correlated phases or exotic quantum criticalities [40, 68–74]. In the twisted MoTe₂ system, a topological transition from $\mathcal{C} = 1$ to $\mathcal{C} = 0$ can be induced by either tuning the twisted angle θ or the displacement field V_z , inducing the possibility of CDW-FCI phase transition. Here, we focus on displacement field $V_z = 2$ meV and tune the twisted angle θ from 2° to 4° .

At $\theta = 2^\circ$, the system is in the CDW phase, and the dispersion of magnetoroton is almost flat and features a sizable gap, except at the commensurate momentum $K, K' + n\mathbf{G}$ where the neutral excitation energy is nearly zero. This means that in the CDW phase, the excitations become soft at those momenta, as can be expected from the fact that the static form factor $\bar{S}(q)$ exhibits peaks at those momenta and suppresses the dispersion. At $\theta = 4^\circ$, the system is in the FCI phase, and the dispersion exhibits a local minimum at finite \mathbf{q} .

We next focus on the long-wavelength excitations. As the angle decreases, the FCI becomes less stable and the highly concentrated peak is broadened, signaling the instability of excitations in Fig. 3(a). The ratio I_+^{\max}/I_-^{\max} between the peak value of opposite chiralities of non-zero energy is evaluated. When the FCI is less stable with a smaller many-body gap, different chirality branches start to mix and the ratio reaches 18.17% at the critical points. The chiral mixing and the broadening spectrum can be interpreted as a new indicator of FCI stability from the perspective of excitations. The deviation from the ideal FCI results in reduced stability of geometrical excitations.

We now dive into the CDW regime, where the band is topologically trivial. We generalize the operator $\hat{\mathcal{O}}$ associated with the geometrical dynamics to a topological trivial band by anisotropy deformation or generally volume-preserving diffeomorphism (VPD) [57, 75], which

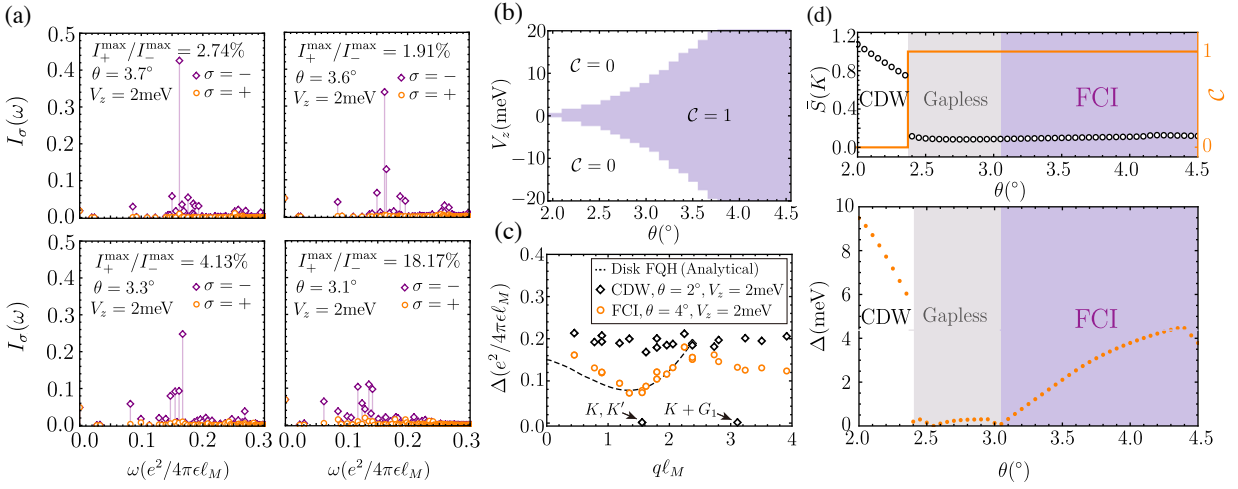


FIG. 3. (a) Comparison between opposite chiral spectral function at different twisted angles θ in FCI phases. (b) Band topology in twisted MoTe_2 as function of displacement field V_z and twisted angle θ . (c)(d) Phase structure indicators at small displacement field $V_z = 2\text{meV}$ as function of twisted angle θ . In (c) the dots are the projected static structure factor $\bar{S}(q)$ at K points that exhibit a peak at CDW phases and are featureless at gapless and FCI phases. The orange line is the Chern number of the top band. In (d) the solid orange dots are the many-body gap from the ED calculations. (c) is the variational energy from SMA at $V_z = 2\text{meV}$ at $\theta = 2^\circ$ (FCI) and $\theta = 4^\circ$ (CDW). At the CDW phase, the magnetoroton is softened at commensurate momentum due to the strongly peaked static structure factor.

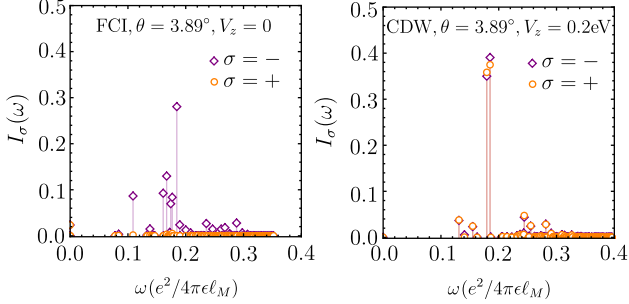


FIG. 4. The spectral weight function of the angular momentum-2 operator coupled to quantum metric for FCI ($\theta = 3.89^\circ$, $V_z = 0$) and CDW ($\theta = 3.89^\circ$, $V_z = 0.2\text{eV}$).

is

$$\sum_{\mathbf{q}, \mathbf{k}, \mathbf{k}'} \frac{V(\mathbf{q})}{2A} \left[(\sigma_z \mathbf{q}) \frac{g_{\mathbf{k}} + g_{\mathbf{k}'}}{2} \mathbf{q}^T \right] \Lambda_{\mathbf{k}, \mathbf{q}} \Lambda_{\mathbf{k}', -\mathbf{q}} \hat{c}_{\mathbf{k}+\mathbf{q}}^\dagger \hat{c}_{\mathbf{k}'-\mathbf{q}}^\dagger \hat{c}_{\mathbf{k}'} \hat{c}_{\mathbf{k}} \quad (6)$$

here $\mathbf{q} = (q_x, q_y)$, $g_{\mathbf{k}}$ is the Fubini-Study metric and $\Lambda_{\mathbf{k}, \mathbf{q}}$ is the form factor. The form of the operator resembles the expression derived in the LLL at the long-wavelength limit when the quantum metric becomes constant [53, 55]. The most important feature of the operator is that it involves the quantum metric of the band instead of Berry curvature, which implies that the geometrical excitations can also emerge in the topological trivial band (see SM Sec. IV for details of geometrical excitations and VPD). At the small displacement field, chiral signals in the spectrum are found in ideal FCIs and the spectrum becomes chiral-mixing and extendedly

distributed with the increasing external field. The excitations remain chiral-mixing and unstable after the system transits into CDW. As shown in Fig. 4, At the strong external field where the underlying topologically trivial band becomes flat, the spectrum exhibits a sharp peak at the $q \rightarrow 0$ extrapolated energy predicted by SMA, representing stable excitations. Moreover, the most prominent feature of the spectrum is that the opposite chiral branches become almost identical, suggesting that the long-wavelength excitations are nonchiral. It is likely to associate the flatness of the band with the stability of excitations, as the strong fluctuation of quantum metric and Berry curvature in the vicinity of phase transition tends to reduce the stability of excitations.

Notice that the nonchiral geometrical excitations have also been unraveled in $\nu = 1/2$ composite fermion liquid (CFL) [53], the nonchiral feature in the flatband CDW might have different roots since CFL is gapless and has particle-hole symmetry. We tentatively assign the non-chirality to the absence of topology. One possible idea is to divide the system into two effective $-\frac{1}{3}$ filled LLLs pierced by the magnetic field of different directions, or equivalently, there might exist two copies of composite fermion feeling opposite residue magnetic field by attaching the equal number of vortices with opposite charge. This may explain why both chiral branches are involved in the neutral excitations. The detailed theoretical analysis of these excitations is left for future studies.

Experiment realizations.— To probe the signal of neutral excitations, it is feasible to apply the resonant inelastic light scattering (RILS) in the twisted MoTe_2 or multilayer graphenes. RILS offers an accessible route to the

Phases	σ_H	\mathcal{C}	Magnetoroton	Chirality
FCI	$\sigma_H = -\frac{2}{3}$	$\mathcal{C} = 1$	stable	chiral
CDW	$\sigma_H = 0$	$\mathcal{C} = 0$	soft at K, K'	nonchiral

TABLE I. Topological indicators, magnetoroton stability and chirality of geometrical excitations of ideal moiré FCI and CDW in flatband.

low-lying neutral excitations in FQH liquids [59, 76] and has recently been applied to detect the interband excitons in the twisted WSe₂ [77]. According to the previous discussion, it is reasonable to identify magnetoroton modes via the recognition of peaks of the density of states at different energies. Besides the magnetorotons predicted previously, it is also likely to find other co-existing excitations, for instance the magnons [78] due to the spin-valley polarized states in FCI phases, or competing excitations which tend to destroy the magnetorotons, for instance, the interband excitations due to the prominent band mixing effects [79]. We leave these possible excitations in the follow-up studies. To capture the features of excitations at the long-wavelength limit, the circularly polarized resonant inelastic light scattering (CP-RILS) [59] is suggested. CP-RILS features in probing the angular momenta of the excitations by measuring the switch of the circular polarizations and thus has the potential to capture the chiral angular momentum-2 nature of the long-wavelength excitations.

Discussions.— In this Letter, we study the magnetorotons in the moiré FCIs, in particular focusing on the twisted MoTe₂. Our study demonstrates that the magnetorotons, serving as the faithful representations of GMP algebra in FQH, also exist in ideal moiré FCIs. Our work suggests the excitations encode the analogous topological order and intrinsic geometric information in FQH and ideal FCI. We also extract necessary information about the excitations when the FCIs are less stable or transit into another phase such as CDW. For instance, there might be chiral-mixing of angular momentum-2 long wavelength excitations for less ideal FCIs. We further find evidence of nonchiral angular momentum-2 excitations at a topological trivial band hosting CDW. We believe that the geometrical excitations can exist without the topology, as geometry and topology serve as two perspectives of the system. Still, the intriguing interplay with topology endows the geometrical excitations with chirality as in FCIs and FQHs. Since some of those observations are beyond the established physics in FQHs and ideal FCIs, they might be beneficial for establishing the unifying theoretical framework of the fractionally filled phases and understanding the phenomena in experiments where the systems are less ideal.

Acknowledgements.— X.S is thankful for the related stimulating discussion with Erez Berg, Lingjie Du, Yiyang Jiang, Dam Thanh Son, Yuzhu Wang, Zhengzhi

Wu, Bo Yang, and Kun Yang, and is especially grateful for the helpful discussion on the experiment realizations with Lingjie Du. This work was supported by the Basic Science Center Project of NSFC (Grant No. 52388201), the National Natural Science Foundation of China (Grant Nos. 12334003, 12421004 and 12361141826), the National Science Fund for Distinguished Young Scholars (Grant No. 12025405), and the National Key Basic Research and Development Program of China (Grant No. 2023YFA1406400).

* These authors contributed equally to the work.

† chongwang@mail.tsinghua.edu.cn

‡ duanw@tsinghua.edu.cn

§ yongxu@mail.tsinghua.edu.cn;

- [1] Y. Cao, V. Fatemi, S. Fang, K. Watanabe, T. Taniguchi, E. Kaxiras, and P. Jarillo-Herrero, Unconventional superconductivity in magic-angle graphene superlattices, *Nature* **556**, 43 (2018).
- [2] Y. Cao, V. Fatemi, A. Demir, S. Fang, S. L. Tomarken, J. Y. Luo, J. D. Sanchez-Yamagishi, K. Watanabe, T. Taniguchi, E. Kaxiras, *et al.*, Correlated insulator behaviour at half-filling in magic-angle graphene superlattices, *Nature* **556**, 80 (2018).
- [3] H. Li, Z. Xiang, E. Regan, W. Zhao, R. Sailus, R. Banerjee, T. Taniguchi, K. Watanabe, S. Tongay, A. Zettl, *et al.*, Mapping charge excitations in generalized wigner crystals, *Nature nanotechnology*, 1 (2024).
- [4] E. C. Regan, D. Wang, C. Jin, M. I. Bakti Utama, B. Gao, X. Wei, S. Zhao, W. Zhao, Z. Zhang, K. Yumigeta, *et al.*, Mott and generalized wigner crystal states in wse₂/ws₂ moiré superlattices, *Nature* **579**, 359 (2020).
- [5] Y. Xie, A. T. Pierce, J. M. Park, D. E. Parker, E. Khalaf, P. Ledwith, Y. Cao, S. H. Lee, S. Chen, P. R. Forrester, *et al.*, Fractional chern insulators in magic-angle twisted bilayer graphene, *Nature* **600**, 439 (2021).
- [6] Y. Xie, B. Lian, B. Jäck, X. Liu, C.-L. Chiu, K. Watanabe, T. Taniguchi, B. A. Bernevig, and A. Yazdani, Spectroscopic signatures of many-body correlations in magic-angle twisted bilayer graphene, *Nature* **572**, 101–105 (2019).
- [7] A. L. Sharpe, E. J. Fox, A. W. Barnard, J. Finney, K. Watanabe, T. Taniguchi, M. Kastner, and D. Goldhaber-Gordon, Emergent ferromagnetism near three-quarters filling in twisted bilayer graphene, *Science* **365**, 605 (2019).
- [8] M. Serlin, C. Tschirhart, H. Polshyn, Y. Zhang, J. Zhu, K. Watanabe, T. Taniguchi, L. Balents, and A. Young, Intrinsic quantized anomalous hall effect in a moiré heterostructure, *Science* **367**, 900 (2020).
- [9] M. Yankowitz, S. Chen, H. Polshyn, Y. Zhang, K. Watanabe, T. Taniguchi, D. Graf, A. F. Young, and C. R. Dean, Tuning superconductivity in twisted bilayer graphene, *Science* **363**, 1059 (2019).
- [10] L. Wang, E.-M. Shih, A. Ghiotto, L. Xian, D. A. Rhodes, C. Tan, M. Claassen, D. M. Kennes, Y. Bai, B. Kim, *et al.*, Correlated electronic phases in twisted bilayer transition metal dichalcogenides, *Nature materials* **19**, 861 (2020).

- [11] Y. Xu, S. Liu, D. A. Rhodes, K. Watanabe, T. Taniguchi, J. Hone, V. Elser, K. F. Mak, and J. Shan, Correlated insulating states at fractional fillings of moiré superlattices, *Nature* **587**, 214 (2020).
- [12] X. Huang, T. Wang, S. Miao, C. Wang, Z. Li, Z. Lian, T. Taniguchi, K. Watanabe, S. Okamoto, D. Xiao, *et al.*, Correlated insulating states at fractional fillings of the ws_2/wse_2 moiré lattice, *Nature Physics* **17**, 715 (2021).
- [13] C. Jin, Z. Tao, T. Li, Y. Xu, Y. Tang, J. Zhu, S. Liu, K. Watanabe, T. Taniguchi, J. C. Hone, *et al.*, Stripe phases in wse_2/ws_2 moiré superlattices, *Nature Materials* **20**, 940 (2021).
- [14] C. Nayak, S. H. Simon, A. Stern, M. Freedman, and S. Das Sarma, Non-abelian anyons and topological quantum computation, *Reviews of Modern Physics* **80**, 1083 (2008).
- [15] A. Y. Kitaev, Fault-tolerant quantum computation by anyons, *Annals of physics* **303**, 2 (2003).
- [16] R. Roy, Band geometry of fractional topological insulators, *Phys. Rev. B* **90**, 165139 (2014).
- [17] N. Regnault and B. A. Bernevig, Fractional chern insulator, *Physical Review X* **1**, 021014 (2011).
- [18] X.-L. Qi, Generic wave-function description of fractional quantum anomalous hall states and fractional topological insulators, *Phys. Rev. Lett.* **107**, 126803 (2011).
- [19] T. S. Jackson, G. Möller, and R. Roy, Geometric stability of topological lattice phases, *Nature Communications* **6**, 10.1038/ncomms9629 (2015).
- [20] S. A. Parameswaran, R. Roy, and S. L. Sondhi, Fractional quantum hall physics in topological flat bands, *Comptes Rendus. Physique* **14**, 816–839 (2013).
- [21] J. Wang, J. Cano, A. J. Millis, Z. Liu, and B. Yang, Exact landau level description of geometry and interaction in a flatband, *Phys. Rev. Lett.* **127**, 246403 (2021).
- [22] C. Wang, X. Shen, R. Guo, C. Wang, W. Duan, and Y. Xu, Fractional chern insulators in moiré flat bands with high chern numbers (2024), [arXiv:2408.03305 \[cond-mat.str-el\]](https://arxiv.org/abs/2408.03305).
- [23] A. P. Reddy, N. Paul, A. Abouelkomsan, and L. Fu, Non-abelian fractionalization in topological minibands, *Phys. Rev. Lett.* **133**, 166503 (2024).
- [24] C.-E. Ahn, W. Lee, K. Yananose, Y. Kim, and G. Y. Cho, Non-abelian fractional quantum anomalous hall states and first landau level physics of the second moiré band of twisted bilayer $mote_2$, *Phys. Rev. B* **110**, L161109 (2024).
- [25] H. Li, U. Kumar, K. Sun, and S.-Z. Lin, Spontaneous fractional Chern insulators in transition metal dichalcogenide moiré superlattices, *Physical Review Research* **3**, L032070 (2021), [arXiv:2101.01258 \[cond-mat.mes-hall\]](https://arxiv.org/abs/2101.01258).
- [26] T. Devakul, V. Crépel, Y. Zhang, and L. Fu, Magic in twisted transition metal dichalcogenide bilayers, *Nature Communications* **12**, 6730 (2021), [arXiv:2106.11954 \[cond-mat.mes-hall\]](https://arxiv.org/abs/2106.11954).
- [27] A. Abouelkomsan, Z. Liu, and E. J. Bergholtz, Particle-hole duality, emergent fermi liquids, and fractional chern insulators in moiré flatbands, *Phys. Rev. Lett.* **124**, 106803 (2020).
- [28] C. Repellin and T. Senthil, Chern bands of twisted bilayer graphene: Fractional chern insulators and spin phase transition, *Phys. Rev. Res.* **2**, 023238 (2020).
- [29] P. Wilhelm, T. C. Lang, and A. M. Läuchli, Interplay of fractional chern insulator and charge density wave phases in twisted bilayer graphene, *Phys. Rev. B* **103**, 125406 (2021).
- [30] H. Goldman, A. P. Reddy, N. Paul, and L. Fu, Zero-field composite fermi liquid in twisted semiconductor bilayers, *Phys. Rev. Lett.* **131**, 136501 (2023).
- [31] P. J. Ledwith, A. Vishwanath, and D. E. Parker, Vortexability: A unifying criterion for ideal fractional chern insulators, *Phys. Rev. B* **108**, 205144 (2023).
- [32] C. Wang, X.-W. Zhang, X. Liu, Y. He, X. Xu, Y. Ran, T. Cao, and D. Xiao, Fractional chern insulator in twisted bilayer $mote_2$, *Physical Review Letters* **132**, 036501 (2024).
- [33] J. Cai, E. Anderson, C. Wang, X. Zhang, X. Liu, W. Holtzmann, Y. Zhang, F. Fan, T. Taniguchi, K. Watanabe, Y. Ran, T. Cao, L. Fu, D. Xiao, W. Yao, and X. Xu, Signatures of fractional quantum anomalous hall states in twisted $mote_2$, *Nature* **622**, 63 (2023).
- [34] H. Park, J. Cai, E. Anderson, Y. Zhang, J. Zhu, X. Liu, C. Wang, W. Holtzmann, C. Hu, Z. Liu, T. Taniguchi, K. Watanabe, J.-H. Chu, T. Cao, L. Fu, W. Yao, C.-Z. Chang, D. Cobden, D. Xiao, and X. Xu, Observation of fractionally quantized anomalous hall effect, *Nature* **622**, 74 (2023).
- [35] F. Xu, Z. Sun, T. Jia, C. Liu, C. Xu, C. Li, Y. Gu, K. Watanabe, T. Taniguchi, B. Tong, J. Jia, Z. Shi, S. Jiang, Y. Zhang, X. Liu, and T. Li, Observation of integer and fractional quantum anomalous hall effects in twisted bilayer $mote_2$, *Phys. Rev. X* **13**, 031037 (2023).
- [36] Z. Lu, T. Han, Y. Yao, A. P. Reddy, J. Yang, J. Seo, K. Watanabe, T. Taniguchi, L. Fu, and L. Ju, Fractional quantum anomalous hall effect in multilayer graphene, *Nature* **626**, 759 (2024).
- [37] K. Kang, B. Shen, Y. Qiu, Y. Zeng, Z. Xia, K. Watanabe, T. Taniguchi, J. Shan, and K. F. Mak, Evidence of the fractional quantum spin hall effect in moiré $mote_2$, *Nature* **628**, 522 (2024).
- [38] Y. Zeng, Z. Xia, K. Kang, J. Zhu, P. Knüppel, C. Vaswani, K. Watanabe, T. Taniguchi, K. F. Mak, and J. Shan, Thermodynamic evidence of fractional chern insulator in moiré $mote_2$, *Nature* **622**, 69 (2023).
- [39] J. Xie, Z. Huo, X. Lu, Z. Feng, Z. Zhang, W. Wang, Q. Yang, K. Watanabe, T. Taniguchi, K. Liu, *et al.*, Even-and odd-denominator fractional quantum anomalous hall effect in graphene moire superlattices (2024), [arXiv preprint arXiv:2405.16944](https://arxiv.org/abs/2405.16944).
- [40] H. Lu, B.-B. Chen, H.-Q. Wu, K. Sun, and Z. Y. Meng, Thermodynamic response and neutral excitations in integer and fractional quantum anomalous hall states emerging from correlated flat bands, *Physical Review Letters* **132**, 10.1103/physrevlett.132.236502 (2024).
- [41] C. Repellin, T. Neupert, Z. Papić, and N. Regnault, Single-mode approximation for fractional chern insulators and the fractional quantum hall effect on the torus, *Physical Review B* **90**, 10.1103/physrevb.90.045114 (2014).
- [42] X. Hu, D. Xiao, and Y. Ran, Hyperdeterminants and composite fermion states in fractional chern insulators, *Phys. Rev. B* **109**, 245125 (2024).
- [43] S. M. Girvin, A. H. MacDonald, and P. M. Platzman, Magneto-roton theory of collective excitations in the fractional quantum hall effect, *Phys. Rev. B* **33**, 2481 (1986).
- [44] W. Kohn, Cyclotron resonance and de haas-van alphen oscillations of an interacting electron gas, *Phys. Rev.* **123**, 1242 (1961).
- [45] S. Mukherjee and S. S. Mandal, Anomalously low magnetoroton energies of the unconventional fractional quan-

- tum hall states of composite fermions, *Phys. Rev. Lett.* **114**, 156802 (2015).
- [46] A. Gromov and D. T. Son, Bimetric Theory of Fractional Quantum Hall States, *Phys. Rev. X* **7**, 041032 (2017), [Addendum: *Phys. Rev. X* **8**, 019901 (2018)], [arXiv:1705.06739 \[cond-mat.str-el\]](#).
- [47] F. D. M. Haldane, E. H. Rezayi, and K. Yang, Graviton chirality and topological order in the half-filled Landau level, *Physical Review B* **104**, 10.1103/physrevb.104.1121106 (2021).
- [48] D. T. Son, Is the composite fermion a Dirac particle?, *Phys. Rev. X* **5**, 031027 (2015).
- [49] F. D. M. Haldane, Self-duality and long-wavelength behavior of the Landau-level guiding-center structure function, and the shear modulus of fractional quantum Hall fluids (2011), [arXiv:1112.0990 \[cond-mat.str-el\]](#).
- [50] A. G. Abanov and A. Gromov, Electromagnetic and gravitational responses of two-dimensional noninteracting electrons in a background magnetic field, *Phys. Rev. B* **90**, 014435 (2014).
- [51] J. Maciejko, B. Hsu, S. A. Kivelson, Y. Park, and S. L. Sondhi, Field theory of the quantum Hall nematic transition, *Phys. Rev. B* **88**, 125137 (2013).
- [52] S.-F. Liou, F. D. M. Haldane, K. Yang, and E. H. Rezayi, Chiral gravitons in fractional quantum Hall liquids, *Phys. Rev. Lett.* **123**, 146801 (2019).
- [53] D. X. Nguyen, F. D. M. Haldane, E. H. Rezayi, D. T. Son, and K. Yang, Multiple magnetorotons and spectral sum rules in fractional quantum Hall systems, *Phys. Rev. Lett.* **128**, 246402 (2022).
- [54] W. Yuzhu and Y. Bo, Geometric fluctuation of conformal Hilbert spaces and multiple graviton modes in fractional quantum Hall effect, *Nature Communications* **14**, 2317 (2023).
- [55] K. Yang, Acoustic wave absorption as a probe of dynamical geometrical response of fractional quantum Hall liquids, *Phys. Rev. B* **93**, 161302 (2016).
- [56] Z. Liu, A. Gromov, and Z. Papić, Geometric quench and nonequilibrium dynamics of fractional quantum Hall states, *Phys. Rev. B* **98**, 155140 (2018).
- [57] Y.-H. Du, U. Mehta, D. Nguyen, and D. T. Son, Volume-preserving diffeomorphism as nonabelian higher-rank gauge symmetry, *SciPost Physics* **12**, 10.21468/scipostphys.12.2.050 (2022).
- [58] A. Pinczuk, B. S. Dennis, L. N. Pfeiffer, and K. West, Observation of collective excitations in the fractional quantum Hall effect, *Phys. Rev. Lett.* **70**, 3983 (1993).
- [59] J. Liang, Z. Liu, Z. Yang, Y. Huang, U. Wurstbauer, C. R. Dean, K. W. West, L. N. Pfeiffer, L. Du, and A. Pinczuk, Evidence for chiral graviton modes in fractional quantum Hall liquids, *Nature* **628**, 78 (2024).
- [60] M. Kang, A. Pinczuk, B. S. Dennis, L. N. Pfeiffer, and K. W. West, Observation of multiple magnetorotons in the fractional quantum Hall effect, *Phys. Rev. Lett.* **86**, 2637 (2001).
- [61] T. M. R. Wolf, Y.-C. Chao, A. H. MacDonald, and J. J. Su, Intra-band collective excitations in fractional Chern insulators are dark (2024), [arXiv:2406.10709 \[cond-mat.str-el\]](#).
- [62] F. Wu, T. Lovorn, E. Tutuc, I. Martin, and A. MacDonald, Topological insulators in twisted transition metal dichalcogenide homobilayers, *Physical Review Letters* **122**, 086402 (2019).
- [63] In practical, the truncation is set to be $3|\mathbf{G}|$ to ensure the convergence of \mathbf{q} summation in practical. In fact, due to the exponential decay of the form factor, the contribution outside the 1st BZ in summation of \mathbf{q} is strongly suppressed, and hence one can directly apply the $(q_x \pm iq_y)^2$ and set the truncation of the summation up to the 1st BZ.
- [64] C. Xu, J. Li, Y. Xu, Z. Bi, and Y. Zhang, Maximally localized Wannier functions, interaction models, and fractional quantum anomalous Hall effect in twisted bilayer MoTe₂, *Proceedings of the National Academy of Sciences* **121**, e2316749121 (2024).
- [65] P. Sharma, Y. Peng, and D. N. Sheng, Topological quantum phase transitions driven by displacement fields in the twisted MoTe₂ bilayers (2024), [arXiv:2405.08181 \[cond-mat.mes-hall\]](#).
- [66] A. P. Reddy, F. Alsallom, Y. Zhang, T. Devakul, and L. Fu, Fractional quantum anomalous Hall states in twisted bilayer MoTe₂ and WSe₂, *Physical Review B* **108**, 085117 (2023).
- [67] X. Shen, C. Wang, R. Guo, Z. Xu, W. Duan, and Y. Xu, Stabilizing fractional Chern insulators via exchange interaction in moiré systems (2024), [arXiv:2405.12294 \[cond-mat.str-el\]](#).
- [68] J. Yu, J. Herzog-Arbeitman, M. Wang, O. Vafek, B. A. Bernevig, and N. Regnault, Fractional Chern insulators versus nonmagnetic states in twisted bilayer MoTe₂, *Physical Review B* **109**, 045147 (2024).
- [69] X.-Y. Song, C.-M. Jian, L. Fu, and C. Xu, Intertwined fractional quantum anomalous Hall states and charge density waves, *Physical Review B* **109**, 115116 (2024).
- [70] H. Lu, H.-Q. Wu, B.-B. Chen, K. Sun, and Z. Y. Meng, Interaction-driven roton condensation in $c = 2/3$ fractional quantum anomalous Hall state (2024), [arXiv:2403.03258 \[cond-mat.str-el\]](#).
- [71] D. Waters, A. Okounkova, R. Su, B. Zhou, J. Yao, K. Watanabe, T. Taniguchi, X. Xu, Y.-H. Zhang, J. Folk, *et al.*, Interplay of electronic crystals with integer and fractional Chern insulators in moiré pentalayer graphene, *arXiv preprint arXiv:2408.10133* (2024).
- [72] L. Bonsall and A. A. Maradudin, Some static and dynamical properties of a two-dimensional Wigner crystal, *Phys. Rev. B* **15**, 1959 (1977).
- [73] T. Tan and T. Devakul, Parent Berry curvature and the ideal anomalous Hall crystal (2024), [arXiv:2403.04196 \[cond-mat.mes-hall\]](#).
- [74] J. Dong, T. Wang, T. Wang, T. Soejima, M. P. Zaletel, A. Vishwanath, and D. E. Parker, Anomalous Hall crystals in rhombohedral multilayer graphene I: Interaction-driven Chern bands and fractional quantum Hall states at zero magnetic field (2024), [arXiv:2311.05568 \[cond-mat.str-el\]](#).
- [75] H. La, Area preserving diffeomorphisms and 2-d gravity (1995), [arXiv:hep-th/9510147 \[hep-th\]](#).
- [76] C. F. Hirjibehedin, I. Dujovne, A. Pinczuk, B. S. Dennis, L. N. Pfeiffer, and K. W. West, Splitting of long-wavelength modes of the fractional quantum Hall liquid at, *Physical Review Letters* **95**, 10.1103/physrevlett.95.066803 (2005).
- [77] N. Saigal, L. Klebl, H. Lambers, S. Bahmanyar, V. Anić, D. M. Kennes, T. O. Wehling, and U. Wurstbauer, Collective charge excitations between moiré minibands in twisted WSe₂ bilayers probed with resonant inelastic light scattering, *Physical Review Letters* **133**, 046902 (2024).
- [78] T. Wang, T. Devakul, M. P. Zaletel, and L. Fu, Diverse

- magnetic orders and quantum anomalous hall effect in twisted bilayer mote_2 and wse_2 (2024), arXiv:2306.02501 [cond-mat.str-el].
- [79] J. Yu, J. Herzog-Arbeitman, M. Wang, O. Vafek, B. A. Bernevig, and N. Regnault, Fractional chern insulators vs. non-magnetic states in twisted bilayer mote_2 (2023), arXiv:2309.14429 [cond-mat.mes-hall].